Appendix for

Deficiency in the nuclear long noncoding RNA *Charme* causes myogenic defects and heart remodeling in mice

Monica Ballarino, Andrea Cipriano, Rossella Tita, Tiziana Santini, Fabio Desideri, Mariangela Morlando, Alessio Colantoni, Claudia Carrieri, Carmine Nicoletti, Antonio Musarò, Dònal O' Carroll and Irene Bozzoni.

CONTENTS:

Appendix Figure S1

A

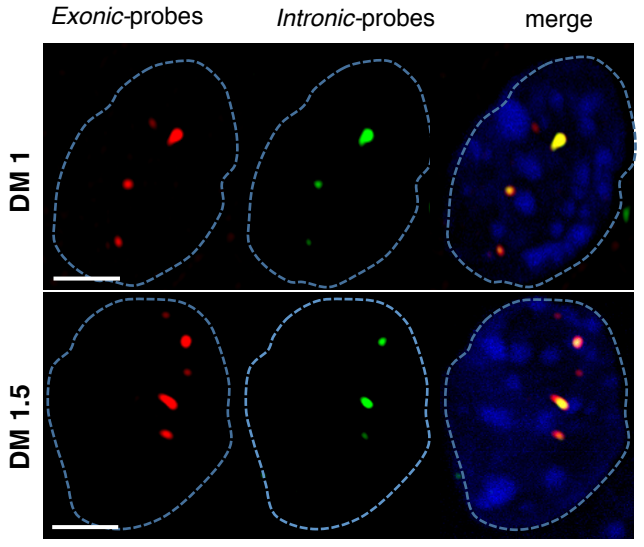

Spots	GM	DM 1	DM 1.5
Exonic	-	4,14 ± 1,7	4,7 ± 1,7
Intronic	-	2,6 ± 0,2	2,6 ± 0,7

B

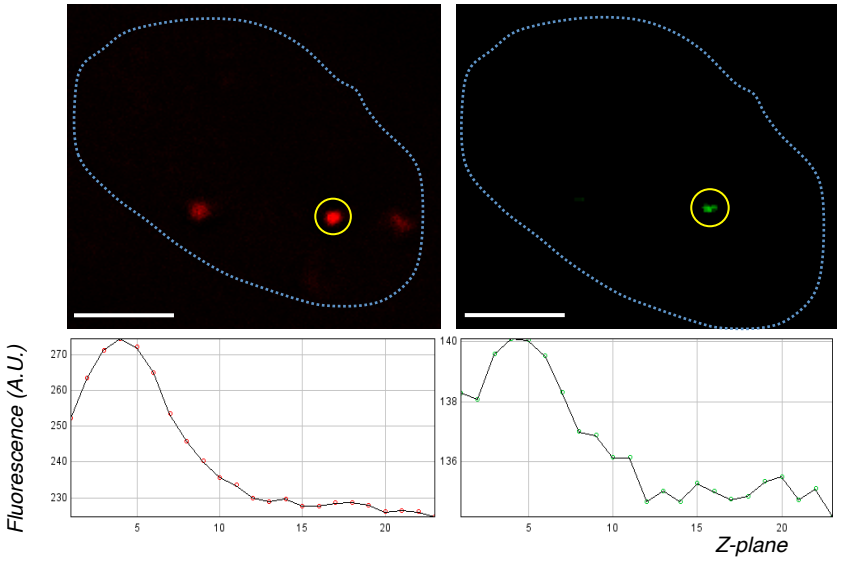

C

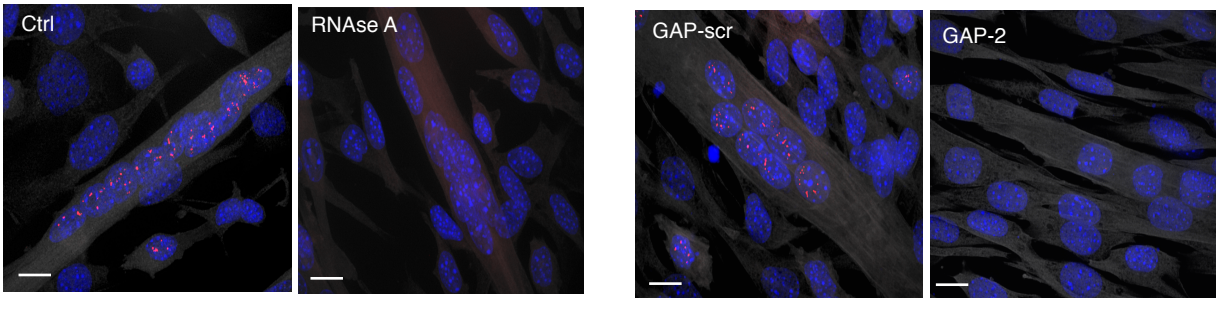

Appendix Figure S1

(**A**) Double RNA FISH showing the location of *Charme* RNA in C_2C_{12} nuclei. Positioning of RNA FISH probes is shown in Fig 1A. Exonic probes visualize both spliced and unspliced molecules (red) while intronic probes detect the precursor molecules (green). Yellow spots indicate overlaps between exonic and intronic signals. The quantification of exonic or intronic spots is shown below. The number±SD of spots per cells was counted from (at least) 100 asynchronous cells nuclei. Images correspond to 2D maximum intensity projection of confocal Z-stacks. In blue the DAPI staining. To note, there are three red/green RNA spots per nuclei. It reflects the C_2C_{12} aneuploidy that contain three copies of chromosome 7 (**B**) Z-axis profile graph. The original Z-stacks of double FISH staining (red: exonic stain; green: intronic stain) were splitted into the corresponding colour channels and analyzed with ImageJ to visualize the Fluorescence intensity profile (A.U.= Arbitrary Units) along the Z-plane. The images show individual focal planes of Z-stack (slice 4), corresponding to the mean maximum value of the co-localized signals. (**C**) RNA FISH controls. Left: effect of RNase A treatment on *Charme* signals. No signal was detected when RNAse A was added prior hybridization, indicating that the probes are specific for RNA. Right: effect of GAP-2 treatment on *Charme* signals. GAP-2 treated samples show a strong reduction of the exonic signals, indicating the specificity of the probes for *Charme*. Scale bar=5μm in (**A**) and (**B**), 10μm in (**C**).

Appendix Figure S2

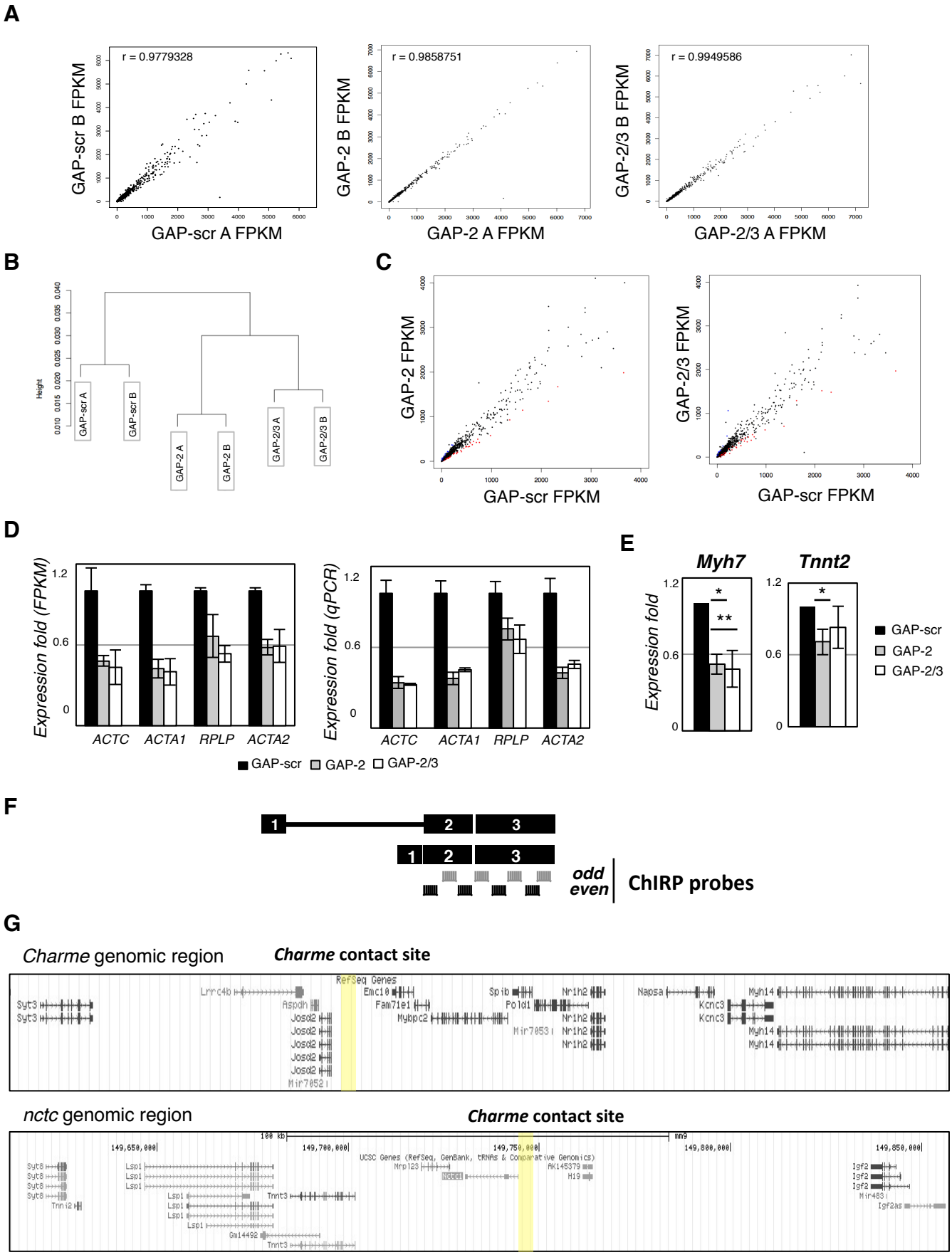

Appendix Figure S2

(**A**) Scatter-plot showing the correlation between the FPKM values obtained for each gene in the two RNA-Seq replicates (A and B) of each condition (GAP-scr, GAP-2 and GAP-2/3). Gene expression shows a high degree of correlation in each pair of biological replicates. r=Pearson correlation coefficient. (**B**) Hierarchical clustering of RNA-Seq replicates (A and B) of each condition (GAP-scr, GAP-2 and GAP-2/3) samples based on the Pearson's correlation of global gene expression. (**C**) Scatter-plot showing the correlation between the FPKM values obtained for each gene in the two RNA-Seq conditions (GAP-scr *vs* GAP-2 and GAP-scr *vs* GAP-2/3). Genes upregulated (blu), downregulated (red) and not affected (black) by *Charme* depletion are shown. (**D**) Validation of top-ranked genes with significant differential expression in *Charme* knock-down RNA-seq. FPKM (RNA-seq) and qRT-PCR expression values are presented as an average±SD of two biological replicates. (**E**) qRT-PCR analyses of *Myh7* and *Tnnt2* mRNA transcripts in cells transfected with GAP-2 or GAP-2/3 compared to GAP-scr control. *P<0.05, **P<0.01, ***P<0.001 unpaired Student's t-test. (**F**) Schematic representation of *Charme* isoforms with the "even" (black) and "odd" (grey) antisense biotinylated DNA probes used in ChIRP. Oligos complementary to lacZ RNA were used as control. (**G**) *Charme* locus and its main interacting genomic target (*nctc*); The regions corresponding to ChIRP-seq peaks are highlighted in yellow.